[Mansoura Engineering Journal](https://mej.researchcommons.org/home)

Volume 48 | Issue 2 Article 2

May 2023

Probabilistic Assessment of Power Systems Resilience Under Natural Disasters

Enas M. Hegazy
Electrical Eng. Dept., Faculty of Engineering, Mansoura University, El-Mansoura, Egypt.

Abdelfattah A. Eladl
Electrical Eng. Dept., Faculty of Engineering, Mansoura University, El-Mansoura, Egypt., eladle7@mans.edu.eg

Magdi M. El-Saadawi
Electrical Eng. Dept., Faculty of Engineering, Mansoura University, El-Mansoura, Egypt.

ORIGINAL STUDY

Probabilistic Assessment of Power Systems Resilience Under Natural Disasters

Enas M. Hegazy, Abdelfattah A. Eladl*, Magdi M. El-Saadawi

Department of Electrical Engineering, Faculty of Engineering, Mansoura University, El-Mansoura, Egypt

Abstract

Extreme weather can have a substantial influence on a power system's operational resilience since they are high-impact, low-probability (HILP) events. Therefore, power systems must be resilient to HILP incidents in addition to being reliable against widely spread and credible threats. Despite the rarity of such events, the severity of their potential impact necessitates the development of appropriate resilience assessment tools to capture their implications and enhance the resilience of energy infrastructure systems. In this paper, a probabilistic strategy is proposed to assess and evaluate the operational resilience of power distribution networks against the impacts of HILP events depending on value-at-risk and conditionally value-at-risk quantitative risk-based assessments. With several scenarios built on sequentially Monte Carlo simulations, the consequence of a windstorm on a distribution network can be assessed using a probability-based resilience assessment methodology. The presented method is examined on an IEEE 37-bus system. Different case studies based on detailed data are presented and analyzed to demonstrate the proposed method's usefulness.

Keywords: Conditional value at risk, Distribution system resilience high-impact, Low-probability events, Extreme weather, Value at risk

1. Introduction

Extreme weather events can cause major power shortages or blackouts. Many power system researches were developed to focus on high-impact, low-probability (HILP) events like storms, severe ice, and flooding. The ability of a power system to reduce the risk of blackouts or extensive power outages caused by HILP occurrences is referred to as its resilience. Distribution networks are the parts of the electrical power systems that are most vulnerable to natural disasters. Distribution networks account for around 90% of all hurricane-related disruptions (Executive Office of the President of the United States, 2013). In a resilient power system, the rate of unserved loads decreases as HILP event intensity rises. According to the Electricity Generation Company of Malawi, Tropical Storm Ana in Southern Malawi, produced catastrophic flooding in several districts of Malawi, particularly in the Southern Region. That happen owing to heavy rainfall and high winds on January 26, 2022 (Friederike et al., 2022). Damage to electricity transmission lines (132 kV and 66 kV), distribution infrastructure (poles, broken jumpers, and conductors), and generating stations resulted in a reduction in power generation. A 271 MW of generation capacity was lost from hydropower units at Nkula, Tedzani, and Kapichira. Additionally, over half of the country's entire capacity of 537 MW according to the Electricity Generation Company of Malawi was cut off.

Due to the obvious connection between power system resilience and HILP occurrences, there are many alternatives, imprecise, and confusing resilience definitions in power system literature (Arghandeh et al., 2016). There is not yet a globally recognized definition, to the best of the authors' information. The most often used definitions were presented in (Arghandeh et al., 2016; Gholami et al.,

Received 12 December 2022; revised 26 February 2023; accepted 22 March 2023.
Available online 18 May 2023

* Corresponding author at: Abdelfattah A. Eladl, PhD, Department of Electrical Engineering, Faculty of Engineering, Mansoura University, El-Mansoura, 35516, Egypt. Tel.: +201227074312.
E-mail address: eladle7@mans.edu.eg (A.A. Eladl).

https://doi.org/10.58491/2735-4202.3032

2018; Stankovic, 2018; McGranaghan et al., 2013; Khodaei, 2014; Parhizi et al., 2015). Although there is no agreement in the literature on the resilience components, there are three resilience components described in (Obama, 2013; Fisher et al., 2010; Ji et al., 2017): withstand, adaptation, and recovery. Withstand means the ability to resist extreme events. Adaptation is the ability to reduce the impact during a disaster. The recovery is the capability to quickly restore system performance to the predisaster state. To evaluate electricity outages many researchers have modified current reliability metrics, such as the system average interruption duration index (SAIDI), the system average interruption frequency index (SAIFI), and the customer average interruption duration index (CAIDI) (Brown et al., 2012). Additionally, the expected energy not supplied (EENS) is used to calculate the restoration capability of a distribution system (Lopez et al., 2016). However, these measures are created for outages that fall under the N-1 or N-2 failure types and do not include the significant failure brought on by HILP occurrences (Liu, 2015). Furthermore, extreme weather-related disruptions prioritize serving vital loads (Coffey et al., 2015), so reliability measurements cannot be applied to access resilience. This is because the capacity for survival is what separates resilience from reliability. The capacity for survival means the ability of a system to continue providing services to consumers despite a disruption (Coffey et al., 2015).

Multiple approaches have been suggested in related literature to calculate the power system's resiliency and robustness. In (Wang and Wang, 2015), a method for minimizing operational costs while maximizing profits was presented. The outputs of distributed generators (DGs) were controlled using a rolling-horizon optimization method. That is based on forecasts during the fault clearance period. But, in that study, the fault locations were predetermined and easy load pickup was presumed, so HILP event effects were not properly modelled. However, the work in (Khodaei, 2014) aimed to minimize the microgrid (MG) load curtailment by effectively scheduling available resources when the main grid supply was disrupted for an extended period. The transition of MG from normal to islanded functioning was not modeled and fault occurrence and repair time was just assumed. So, the paper does not precisely reflect the probabilistic character of HILP occurrences.

Furthermore, the restoration approach in (Chen et al., 2018) depended on a set of control operations that integrated switches, DGs, and switchable loads. That is for creating numerous isolated MGs in the event of major network disruptions. Again, in that paper, climatic occurrences were not modelled, although the preexistent faults caused by weather events were considered. The study in (Lei et al., 2018) utilized mobile generators as DGs for resilient load restoration through MG formation. Although a model with two stages was employed it could preposition mobile generators in the best possible locations and allocate them in real-time. However, the road network damage was not taken into consideration and the uncertainty of storm occurrences and their fluctuating conditions were ignored. In (Lin and Bie, 2018), the hardening strategy for a distribution system under malicious attacks was determined using a tri-level defender-attacker-defender (DAD) model. The system defender made decisions on hardening on the initial level. The attacker located the attack scenario that might cause the most damage on the second level. On the third level, the system operator implemented resilient operational measures, using DG islanding formation and topology reconfiguration. However, that research took into account weighted load shedding, algorithm processing took a long time. Moreover, preexisting defects induced by weather occurrences were assumed and weather events themselves were not modelled.

To overcome the drawbacks of the aforementioned methods, this research introduces probabilistic measure indexes to estimate the electrical power distribution networks' operational resilience for HILP events. Using two risk-based metrics, value-at-risk ($VaR\alpha$) and conditional-value-at-risk ($CVaR\alpha$). They assess the resilience of the distribution network by determining the maximum loss of energy and the conditional expectation of a loss of energy, respectively. The presented metrics will give a preview of the effects that a future HILP incident might have. These metrics study the influence of an occurrence on the delivery and operation of the electricity system (in terms of MWh not served). And they can evaluate the system's anticipated performance during a severe event. They can also calculate the impact on long-term assets. Consequently, this method considers a resilience-enhancing measure as it estimates the impact of robust strategy on distribution system resilience.

The major contributions of this paper are as follows:

(1) A fragility model of the distribution system infrastructures (lines, towers, and transformers) is constructed to examine the influence of severe weather conditions on the resilience of the distribution network and assess resistance to

extreme windstorms. The effects of storms or any other heavy calamities on electric networks are estimated using component-level fragility curves.
(2) The Monte-Carlo simulation is used to generate damage scenarios and develop system-level impact and calculate the load loss (MW) in each weather event.
(3) Two risk-based indicators VaRα and CVaRα, determine both the maximum loss of energy and the conditional expectation of experiencing a system loss (in MWh). These indicators evaluate the anticipated decrease caused by the events with the biggest impact. Specifically, the events occur above a specified risk threshold, α.
(4) The impacts of robust techniques on improving the resilience of the electrical distribution system are computed and described, in order to reduce the probable loss and improve the system's resilience.
(5) The most important contribution of this paper is to propose a novel method that can help planners to predict and appropriate system infrastructure upgrades to reduce the impact of an impending extreme occurrence on the system's important loads.

The rest of this paper is organized as follows. Section 2 discusses the definitions of the proposed resilience metrics, explains system performance loss and probabilistic events, and presents resilience metrics based on risk. Section 3 presents the component-level effect model, and analyzes fragility modeling and resilience evaluation of the main distribution components. In Section 4, the system-level impact model is derived, the resilience curve and system performance are represented visually, and the impacts of the hardening planning model and system performance losses are discussed. Section 5 proposed a detailed simulation framework for quantifying resilience. Section 6 presents and analyzes the results of applying the proposed method on the IEEE 37-bus test system to clarify the idea of resilience assessment. Finally, section 7 concludes the whole paper.

2. Problem formulation

To assess the effects of HILP events on distribution system performance and to estimate the risks posed by such occurrences on system resilience, a framework based on Monte Carlo simulation studies is provided. By simulating varying degrees of damage to distribution networks and the effects of hardening procedures, resilience is measured based on the proposed metrics. This section begins with defining the proposed resilience metrics. The system performance loss under probabilistic event is modeled and finally, the resilience metrics based on risk are derived.

2.1. Definitions of proposed resilience metrics

The metrics value-at-risk (VaR) and conditional value-at-risk (CVaR) have been extensively used in risk-averse financial planning to manage the impacts of low-probability high-risk financial investments. Similar factors come into play when controlling the effects of HILP occurrences, making these metrics useful for quantifying both possible harms and potential benefits of alternative planning efforts. The suggested resilience indicators were inspired by the literature on risk management that deals with measuring the risks associated with a specific economic investment. In light of this, risk-based resilience indicators are used to quantify how resilient the power distribution networks are toward the effects of extreme occurrences. The stated method determines the effects of an incident on the operation of the power system (in terms of MWh not served). It demonstrates the probable effects of forthcoming HILP events and assesses the system's predicted performance during a severe occurrence like a storm. In this context, the two measures VaRα and CVaRα are frequently employed in the literature of risk management to assess the effects of the events with low probability that may result in extremely high system losses. A well-liked approach for controlling risk is CVaR, which was first developed by Rockafellar and Uryasev (2000). Conditional value at risk is derived from the value at risk for a portfolio or investment.

The VaR cutoff point is the starting point for calculating CVaR, which is calculated by averaging the weighted ‘extreme‘ losses that lie in the tail of the distribution of potential returns. When optimizing a portfolio, CVaR is utilized to manage risk effectively. Utilizing CVaR as opposed to VaR alone typically results in a more conservative approach to risk exposure. Both metrics are best suited to quantify operational resilience since they precisely quantify the high losses resulting from low-probability situations (Bardou et al., 2009). The maximum probable loss is measured by VaRα. And the estimated shortfall caused by the highest impact events that occur beyond a specified risk threshold α is measured by CVaRα as shown in Fig. 1.

In the following subsections, some concepts that are employed to evaluate the suggested resilience

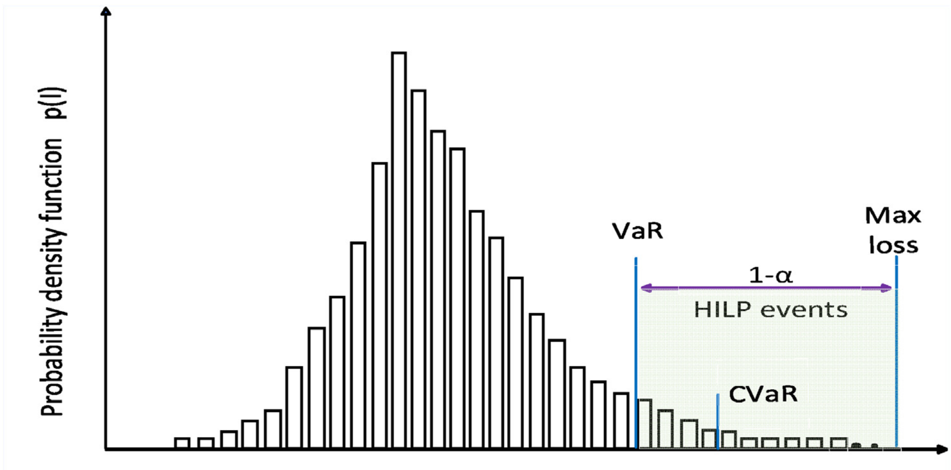

Fig. 1. VaRα and CVaRα for a probabilistic storm event assessment.

indicators for distribution systems subjected to HILP occurrences will be established. The loss in system performance induced by probabilistic interruption events is used to characterize system resilience. To compute this, it is necessary to derive a model of the event's impact on the performance loss function of the system as well as the event probabilistic model.

2.2. System loss and probabilistic event

An event is made up of two components; its chance of happening, *P(i)*, and its intensity, which is a random variable, *(i)*. The probability density function (PDF) of wind speed inside a specific area is shown in Fig. 2. The figure illustrates the characteristics of a storm event for three different places (normal, high, and extreme) wind profiles. In the figure, the x-axis represents the severity of the event (wind speed), and the y-axis represents the probability of the event. The probability that distribution system components (towers, lines, and transformers) may fail is influenced by the event's severity, this ultimately affects how well the system's performance loss. Modeling the effects of a particular natural calamity event on the performance of the distribution network is frequently done using a system performance curve, also referred to as a resilience curve (Panteli et al., 2017a).

When a random event (i) has an influence on a system, the performance loss, $U(i)$, is represented as a nonlinear function of the loss of load $L(i)$. And the total time takes to restore the system to its previous level of performance, $t\,(i)$, as specified in (1) (MacKenzie and Zobel, 2016):

$$U(i) = f(L(i)\; t(i)) \tag{1}$$

Normally, $U(i)$ is determined by calculating the area under the system performance curve, when affected by a random event. It is noted that proactive planning strategies such as distribution line hardening can improve the system performance loss (MacKenzie and Zobel, 2016). These impacts are captured by accurately simulating the system performance curve as described later.

2.3. Resilience metrics based on risk

Initially the performance loss function of the system, $U(i)$, is determined by randomizing the selected events from the $P(i)$, and PDF. The measured loss, $U(i)$, and the likelihood of observing such loss, $P(i)$, are combined to produce the PDF for $U(i)$ as explained in Fig. 1. When a random event, i, has an impact on the system loss, $U(i)$, the probability that it would not surpass a certain threshold ς is given by (2):

$$\psi\,(\varsigma) = \int_{U(i)\leq\varsigma} P(i)\; d(i) \tag{2}$$

where, $\psi\,(\varsigma)$ gives the cumulative distribution function for network losses caused by a storm event (i) with the probability $P(i)$. The value at risk, VaRα, in the range of (0, 1) for a particular probability level α is given by (3).

$$VaR\alpha = min\{\varsigma\, \epsilon R : \psi(\varsigma) \geq \alpha\} \tag{3}$$

The CVaRα metric is the estimated system loss (MWh) resulting from the top $(1-\alpha)\%$ of greatest impact events. Equation (4) can be used to compute

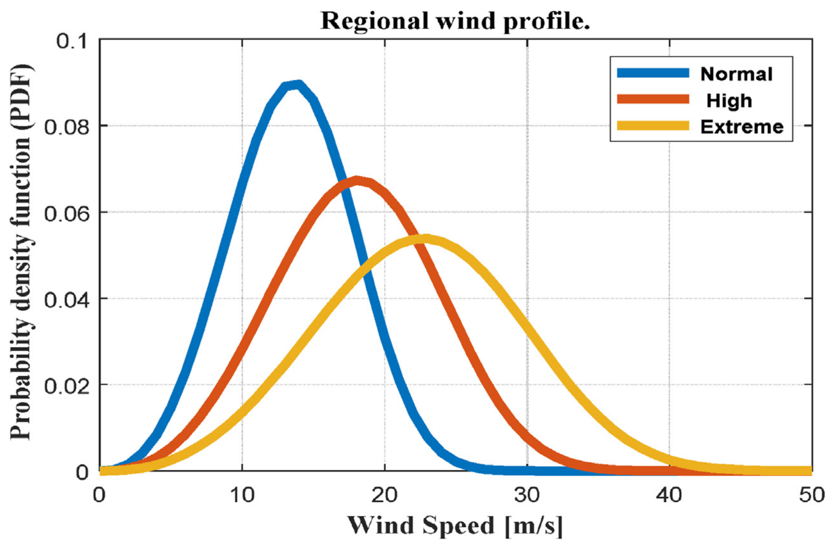

Fig. 2. Probabilistic component-level fragility curve.

the CVaRα metric which will be used to assess the system's resilience. That is by estimating the performance loss brought on by those HILP situations with a high probability (i.e., the ending of the PDF for $U(i)$ given in Fig. 1) (Vugrin et al., 2017).

$$CVaR\alpha = (1-\alpha)^{-1} \int_{U(i)\geq VaR\alpha} U(i)\,P(i)\,d(i) \tag{4}$$

It is important to note that, the whole set of events with probabilities (α) and $(1-\alpha)$ respectively, includes events with losses greater than the stated threshold and others with losses that fall short of the target level.

3. Component-level effect model

High winds have the potential to shatter power lines, transformer damage, and break towers, resulting in widespread power outages. When a weather event influences a system, resilience metrics are proposed before requesting the PDF for loss in system performance [$U(i)$. The PDF for the provided weather event for a specific region is used to calculate the probability of a weather event, $P(i)$. For this, it is initially necessary to estimate the probabilistic influence of a storm event (wind speed) on distribution network components. Three steps can be used to model the storm effect on the distribution system components: determining the most important components of the system, modeling their fragility, and computing the probability of their failure.

3.1. Fragility modeling and resilience evaluation of distribution components

A system model is constructed to examine the influence of severe weather conditions on the resilience of the distribution network. This involves fragility modeling of the distribution system infrastructures as well as assessing resistance to extreme windstorms. The most important components include individual towers, lines, and transformers. Component-level fragility curves are used to estimate the effects of storms or any other heavy calamities on electric networks (Panteli et al., 2017b). A fragility function maps the probability of distribution system component failure regardless of the wind speed (w) of the storm.

3.2. Tower fragility models

A tower fragility indicator predicts the probability of structural component default based on applied stress that reflects the probable severity of a disaster (Kirsty and Bell, 2014; Dunn et al., 2015). The Applied Technology Council's (ATC 58) principles, which were created for the Federal Emergency Management Agency to enhance the structural performance of buildings to seismic hazards, have been redistributed into the methodology. This method is used here to determine the probability that power system towers may fail as a function of wind loading. In order to accurately measure towers' failure probabilities as a function of wind loading, a lognormal distribution is used to describe many structural engineering processes, like strength properties in lab experiments. The lognormal concept determines the probability of being in or surpassing, a damaged state (ds) over a certain level of risk as in (5) (Applied Technology Council, 2018).

$$P\left[ds / S_d\right] = \Phi\left[\frac{1}{\beta_{ds}} ln\left(\frac{S_d}{S_{d,ds}}\right)\right] \tag{5}$$

where $S_{d,ds}$ represents the median value of the engineering demand parameter (e.g., displacement or stress) at which the asset reaches the failure state ds. β_{ds} means the standard deviation of the natural log of the engineering demand parameter during which the asset stretches the damage state ds, and Φ is the normal cumulative distribution function. The fragility curve can be changed depending on the event measurement settings (Panteli and Mancarella, 2017), and the level of incident severity (Nazemi et al., 2020). As an illustration, the failure probability of towers can be represented as a function of wind speed (fragility function) as in (6).

$$P_T(w) = \begin{cases} 0 & w < w_{cr,T} \\ P_{T,hw}(w) & w_{cr,T} < w < w_{co,T} \\ 1 & w > w_{co,T} \end{cases} \tag{6}$$

where $P_T(w)$ denotes tower failure probability as a function of wind speed (w), hw identifies high winds, $w_{cr,T}$ represents the wind speed at which the tower's failure probability increases. The $w_{co,T}$ defines the wind speed at which the tower has a negligible chance of survival (assumed to be 45 m/s and 150 m/s, respectively) (Panteli et al., 2017b). Fig. 3 shows the failure probability of towers with wind speed.

3.3. Modeling line fragility

Topical weather conditions also have an impact on distribution line resilience, which can lead to line failure for a variety of causes, such as shackle breakage. Because line failure is regarded as independent of tower failure, a distinct climate fragility curve is required. Component-level fragility curves were utilized in related research to predict the consequences of hurricanes or other high wind occurrences on electric system components (Lin and Bie, 2018).

The Weibull distribution is usually assumed to describe the fragility curves of overhead power lines (Fang et al., 2019). After that, the line failure probability which reflects the risk of occurrence of distributing network elements depending on the size of the disaster (e.g., a wind speed) can be estimated. The curve seen in Fig. 4, mathematically demonstrates the correlation between the probability of failure of distributing system lines and wind speed as given in (7) (Panteli et al., 2017b):

$$P_L(w) = \begin{cases} {P_L}^n & w < w_{cr,L} \\ P_L(w) & w_{cr,L} < w < w_{co,L} \\ 1 & w > w_{co,L} \end{cases} \tag{7}$$

For which $P_L(w)$ indicates the line failure probability as a wind speed function, ${P_L}^n$ is the point of the rate of failure in good climate circumstances, which is assumed to be 1×10^{-2} (Panteli and Mancarella, 2017) in this case. Meanwhile $w_{cr,L}$ is the wind speed where the line's probability of failure increases, and $w_{co,L}$ is the wind speed at which the line has very little chance of surviving. The values of $w_{cr,L}$ and $w_{co,L}$ are considered equal to 25 and 60 m/s, respectively (Panteli et al., 2017b).

3.4. Modeling transformer fragility

When it comes to attacks or natural disasters, the transformers are essential components. The results are alarming; 70% of large transformers and transmission cables in the network are older than 25 years (Friedman et al., 2012). They are extremely expensive and labor-intensive to replace, with an anticipated lifespan of 40 years. Age increases the probability of failure during regular operations and can increase weather-related outages. For example, Hurricane Ida, in 2021, destroyed over 5900 transformers in the USA (Kasakove, 2021). As a result, the transformer life data will be modelled using the 2-parameter Weibull distribution in this study. The 2-parameter Weibull distribution is the most often used statistical model for lifecycle data analysis of high-voltage power equipment (Melchor-Hernández et al., 2015). Furthermore, a two-parameter Weibull is chosen for its flexibility. This is related to the form parameter of the 2-parameter Weibull resembling the characteristics of other distributions such as the exponential and normal distributions. It is also adaptable in terms of displaying the link between failure rate and failure type. The PDF of the 2-parameter Weibull distribution is given in (8) (Corporation, 2015; Ridwan et al., 2014).

$$F(t) = \frac{\beta}{\eta}\left(\frac{w}{\eta}\right)^{\beta-1} e^{\left(-\frac{w}{\eta}\right)^{\beta}} \tag{8}$$

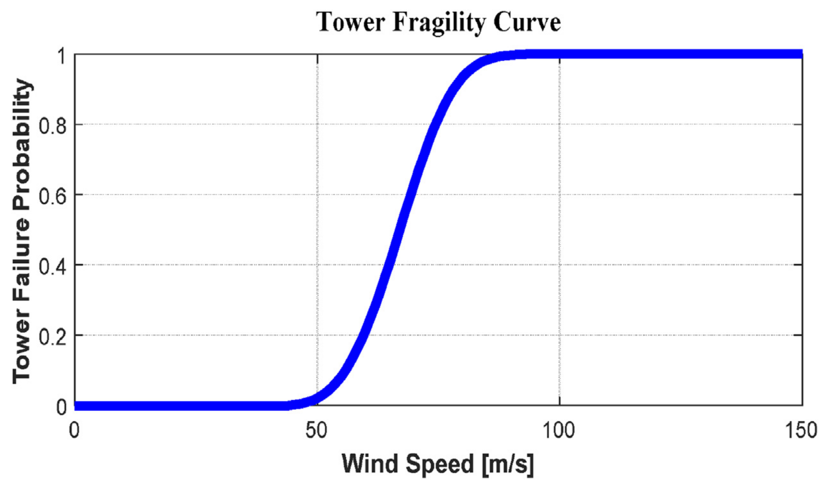

Fig. 3. Tower failure probability.

where β is the shape parameter, and η is the scale parameter. According to actual wind speed data gathered from the northern portion of China (China meteorological data system, 2020), the scale parameter and the shape parameter values are taken as 14 and 2, respectively. The probability density function in life data analysis depicts the failure distribution or frequency of failure as in (9). Fig. 5 displays the relationship between wind speed and the probability that the distribution system transformer may malfunction.

$$P_{tr}(w) = \begin{cases} 0 & w < w_{cr,tr} \\ P_{tr}(w) & w_{cr,tr} < w < w_{co,tr} \\ 1 & w > w_{co,tr} \end{cases} \tag{9}$$

For which $P_{tr}(w)$ indicates the probability of transformer failure as a function of wind speed. The $w_{cr,tr}$ is the wind speed where the transformer's probability of failing increases while $w_{co,tr}$ is the wind speed at which the line has very little chance of surviving. The $w_{cr,tr}$ and $w_{co,tr}$ are considered equal to 50 and 150 m/s, respectively.

3.5. Damage scenarios for components

The occurrence probability of failure of distribution infrastructures (towers, lines, and transformers), $P_{total}(w)$, is used to describe the operational states of specific distribution network components. Each component, *c*, is assigned and uniformly distributed random number, $r_k \sim U(0,1)$ (Harrison, 2010), these random numbers have been contrasted with the event-dependent failure probability $P_{total}(w)$ over the given wind speed, w. Consequently, $FL^c(w)$ determine the component's operational status as in (10).

$$FL^c(w) = \begin{cases} 0 & P_{total}(w) < r_k \\ 1 & P_{total}(w) > r_k \end{cases} \tag{10}$$

where $FL^c(w)$ is the c^{th} component failure function, and $FL^c(w) = 0$ indicates no failure and vice-versa. All components of the distribution networks are collected in their wind-affected operational states. System-level effects and, subsequently, the system loss function, as described in the next section, are determined using the component-level damage.

4. System-level impact model

This section describes the methodology used to simulate how a weather condition may affect the distribution network. Creating a system resilience curve, measuring system performance losses, and modeling proactive planning's effects such as hardening will be discussed.

4.1. Resilience curve and system performance

A basic resilience curve illustrating the many stages in which the power distribution network stays following a catastrophic occurrence is shown in Fig. 6 (Dunn et al., 2015). Events in progress, post-event degraded states, restorative states, and recovery are the phases of that curve and can be defined as follows.

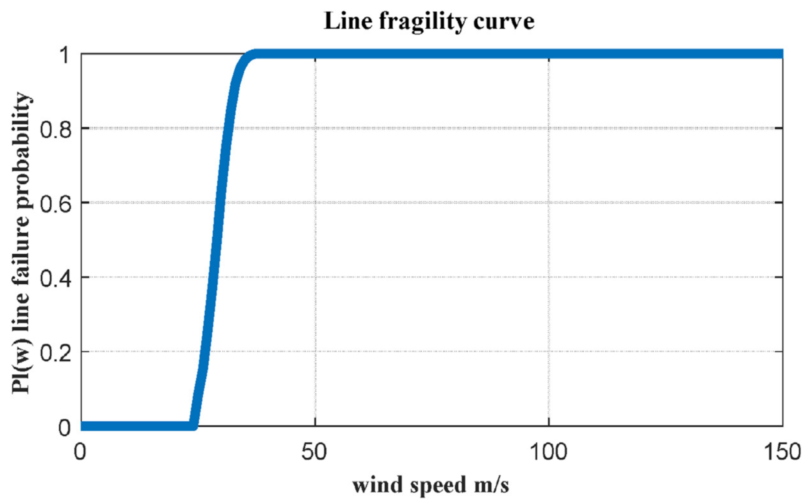

Fig. 4. Line failure probability for a severe event.

(1) Phase I (Event progress): This phase represents the duration of the event (storm), i.e., $t \in [t_e, t_{pe}]$.
(2) Phase II (Post-event degraded state): This phase starts after the event has concluded and ends before any restoration action is done. It involves damage assessment during a period t $\in [t_{pe}, t_r]$.
(3) Phase III (Restoring stage): It represents the restoration automation period and ends before any infrastructure recovery i.e., $t \in [t_r, t_{ir}]$.
(4) Phase IV (Infrastructure recovery stage): In this Infrastructure recovery stage, the system tries to go back to its pre-disaster status and $t \in [t_{ir} - t_{pr}]$.

The simulation methodology for metric calculation is concentrated on the operational resilience metric that is defined by the system performance thought $t_e - t_{ir}$ as depicted in Phases I–II and III. While the infrastructure restoration (phase IV) will not be included in this framework.

4.2. System performance losses

The not served energy (MWh) in the aftermath of a storm was measured as system performance loss, $U(i)$. This is a multi-dimensional concept requiring power losses $L(i)$ along with a transitioning number of hours $t(i)$ required to restore the system to a respectable level. As a result, the system's response during Phases I to III of the resilience curve has a significant impact on operational resilience. The first effect is dependent on the characteristics of the catastrophe. Whenever the network is damaged, for

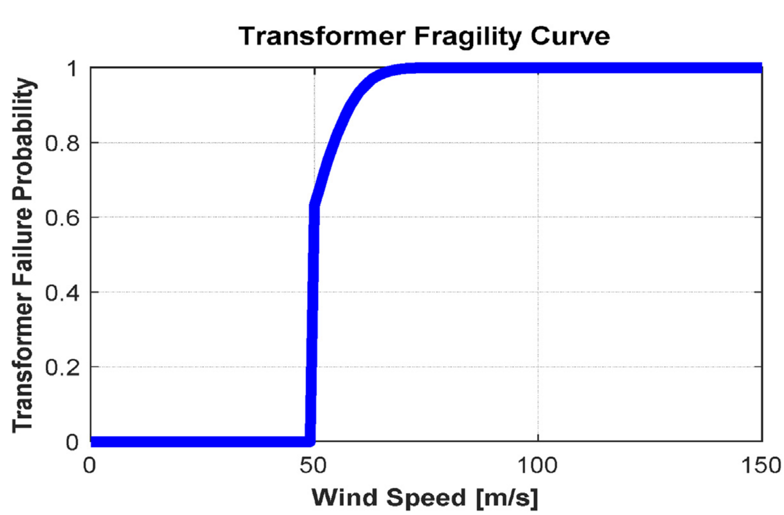

Fig. 5. Transformer failure probability.

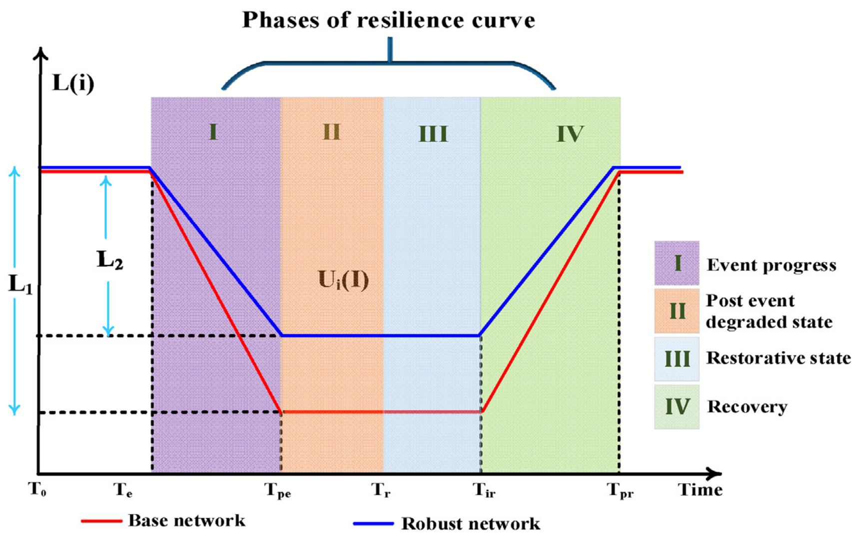

Fig. 6. A basic resilience curve for an incident.

example, by an earthquake its resilience plummets drastically where the duration of the incident ($t \in [t_e, t_{pe}]$). A wind-related disaster, on the other hand, may take much time to damage the system since it travels widely. In the event progress state, service to consumers is paused, and the loss function grows. If the location and timing of a major catastrophe could be correctly predicted, preventive measures can be done before the event to lower $L(i)$. Additionally, reduced system performance loss and/or the slope of degradation resilience can be achieved with enhanced redundancy (as Phase I of Fig. 6).

Let $\tilde{P}$ be a system's unavailability (failure probability) of all system infrastructures and $FL^c(w)$ be a zero-one indication factor of component status. The chance of component c participating in an unsafe operation is stated as follows in (11) for each damage state (i) (Porter et al., 2007).

$$\tilde{P} = \frac{1}{N} \sum_{i=1}^{N} FL^c(w) \tag{11}$$

At which N represents the total of system states tests are performed, then we can calculate the expected load loss, $L(i)$ due to extreme events using (12). The distribution system simulator (OpenDSS) is used to obtain the initial load loss ($LL_{Initial}$) of the distribution system.

$$L(i) = \tilde{P} * LL_{Initial} \tag{12}$$

The area under the resilience curve from t_e to t_{ir}, when affected by an event i, provides the system performance loss, $U(i)$ as shown in Fig. 6. The system performance loss for the base scenario without any hardening actions would be calculated using (13).

$$U_{base}(i) = \frac{1}{2}\left[\left(t_{ir} - t_{pe}\right) + \left(t_{ir} - t_e\right)\right] L_b \tag{13}$$

The Robust scenario's loss of system performance with hardening lines would be calculated using (14).

$$U_{robust}(i) = \frac{1}{2}\left[\left(t_{ir} - t_{pe}\right) + \left(t_{ir} - t_e\right)\right] L_r \tag{14}$$

where L_b is the average load loss in the base case in (kW), and L_r is the average load loss in the robust case in (kW). The fundamental goal of the hardening solutions is to increase infrastructure resilience, which lowers the initial system loss as the storm begins and develops.

4.3. Impacts of hardening planning model

The distribution system resilience can be improved by implementing several precautionary planning strategies. From a practical perspective, a decision-maker can increase network resilience by inserting resources to reduce average impact $L(i)$ and shorten the time needed for damage evaluation ($t_r - t_{pe}$). Additionally, using enhanced recovery strategies to reduce the effects during the restorative state (t_{ir}—t_r). One of the best ways to safeguard the system from powerful windstorms is to harden the distribution lines, despite the cost. The fundamental goal of the hardening approaches is to increase infrastructure resilience, which lowers $L(i)$, the initial system loss, as the incident starts and progresses. Many approaches are used to make the network more robust like (i) using underground lines, (ii) elevating substations, relocating components to areas with lower flooding risks, (iii) strengthening the components' toughness, and (iv) utilizing redundant transmission tracks and rerouting it to the locations with the lowest vulnerability (Dalton and Mote, 2013; Networks Association, 2011; Overbye et al., 2007; Johnston, 2012).

These hardening actions will affect the distribution system components' fragility curve. Components are made more resistant to the extreme wind profile by lowering the wind-induced damage probability. With this strengthening planning strategy, as seen by the blue curve in Fig. 6, the loss will be decreased, and L_b becomes L_r as the state of the event progresses. This robust planning model will be in the pre-event phase, and it is considered a long-term enhancement plan.

5. A detailed simulation framework for quantifying resilience

The purpose of this paper is to assess a distribution system's resilience to the future, which is exceedingly unusual extreme occurrences. In this section, the authors go into different perspectives about the methodology for calculating the resilience metric by assessing the impact on the probabilistic system. The methodology produces the resilience metrics (*VaRα* and *CVaRα*) based on inputs of meteorological data and a thorough system model. Moreover, the system loss function is produced in the suggested method using the component-level fragility curves. The probabilistic effects of a climate event on the power network are assessed using a simulation of the Monte Carlo method, which is frequently used in large-scale network reliability calculations (Li and Billinton, 2013; Liang and Goel, 1997). This is done because the severity of the

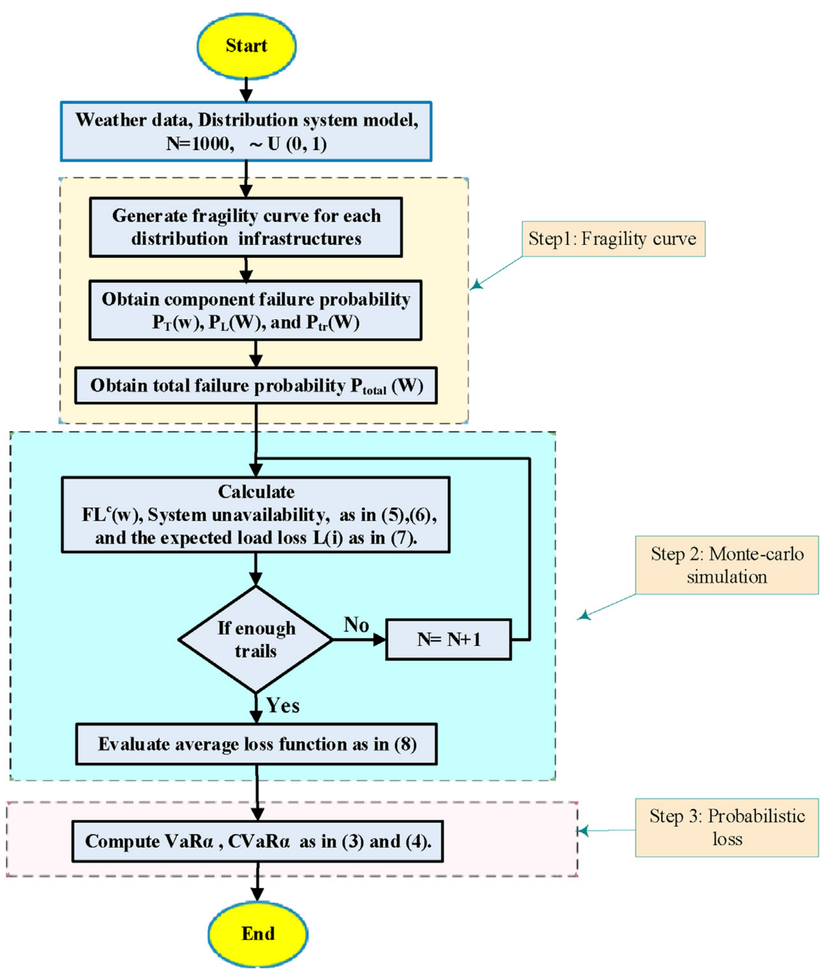

Fig. 7. A flowchart for computing resilience metrics.

weather and how it affects equipment are not deterministic. The Monte Carlo simulations, despite being difficult to solve, are beneficial for the study and design of complex systems, as shown in related important research in this field (Kaygusuz et al., 2014; Paul and Padhy, 2019).

The Monte Carlo method makes it possible to simulate such uncommon occurrences while taking into account the lower chance of doing that. Therefore, it results in a realistic assessment of the hazards related to such HILP events. The procedures for computing resilience metrics have three main steps: fragility modelling, Monte-Carlo simulation, and probabilistic loss as defined in a flowchart in Fig. 7. Also Fig. 8 illustrates the procedure for both base and robust scenarios. The climatic data and a thorough system model are taken as inputs and provide resilience measurements (VaRα and CVaR α).

6. Component fragility modelling

For a certain weather occurrence, the fragility curve is constructed for each distribution component (towers, lines, and transformers), and the PDF of the specified region is taken as explained in Fig. 2 (for the case of wind-related events). After that, the failure probability of each component as seen in Figs. 3−5 and the total failure probabilities of all distribution system infrastructures are obtained. In the case of a hardening scenario by strengthening the distribution overhead lines, the fragility curve will be moved towards the right, helping to make the components more robust to stronger climate events (as clarified in Fig. 8). As a result, the failure probability of the related component is altered when hardening is possible.

6.1. Monte-Carlo simulation

For a specific wind speed, damage scenarios are created using Monte Carlo simulations using the component-level failure probability of all distribution network infrastructures, $P_{total}(w)$. Additionally, the operational condition of the specific component, $FL^c(w)$, is obtained at each trial. Similar steps are taken to determine the operating states of each damage scenario for a certain trial of Monte Carlo. The system loss function is then obtained using the expected load loss $L(i)$. Utilizing the distribution system simulator (OpenDSS) software, the initial load loss$(LL_{Initial})$ is obtained. For different wind speeds, the process is repeated. OpenDSS can analyze a complex electric power distribution network with new load models like electric vehicles, photovoltaic generation, rechargeable battery storage systems, DG resources, and so on.

6.2. Expected loss

Once enough Monte Carlo simulations have been run and for each wind speed sample, the average performance loss expressed in MWh is determined. Then the PDF for loss function is generated as given in Fig. 1 at the finish of the Monte Carlo calculations for all selected wind speeds of the major storm. By mapping the average loss onto the PDF for the particular climate event, a probabilistic representation of the system performance loss brought on by that event is created (wind speed).

Utilizing (3) and (4), the PDF indicating the probabilistic loss function, $U(i)$, is utilized to calculate the VaRα and CVaRα metrics, which can precisely describe and quantify the consequences of HILP occurrences. For a particular level of confidence α, the maximum loss in resilience anticipated over a certain period is calculated by VaRα. Meanwhile, CvaRα estimates the contingent anticipation of seeing a system loss (in MWh) as a result of $(1-\alpha)$% of greatest impact failures.

7. Assessments and results

7.1. IEEE 37-bus test system

In this part, an IEEE-37 test system, shown in Fig. 9, is used to demonstrate the suggested framework. This is a three-phase, unbalanced medium voltage network (4:8 kV) with one main transformer. In this study, Monte Carlo simulations are run on MATLAB R2016a using a PC with Intel(R) Core (TM) i7-8550U CPU@1.80 GHz, 1992 Mhz, 4 Core(s), and 8 Logical Processor(s) RAM.

7.2. Assumptions and environment configuration

This section will describe the simulation processes in detail. For simulation purposes, the following assumptions are considered:

(1) It is expected that no restoration/recovery is undertaken throughout the progression of the event (t_o to t_e) and that all components are working before the event.
(2) In the basic scenario, assume a limited geographical area with uniform weather.
(3) To illustrate preventive disruption-management methods for resilient networks, a random selection of 15 overhead lines to harden in the test system (red lines in Fig. 9).

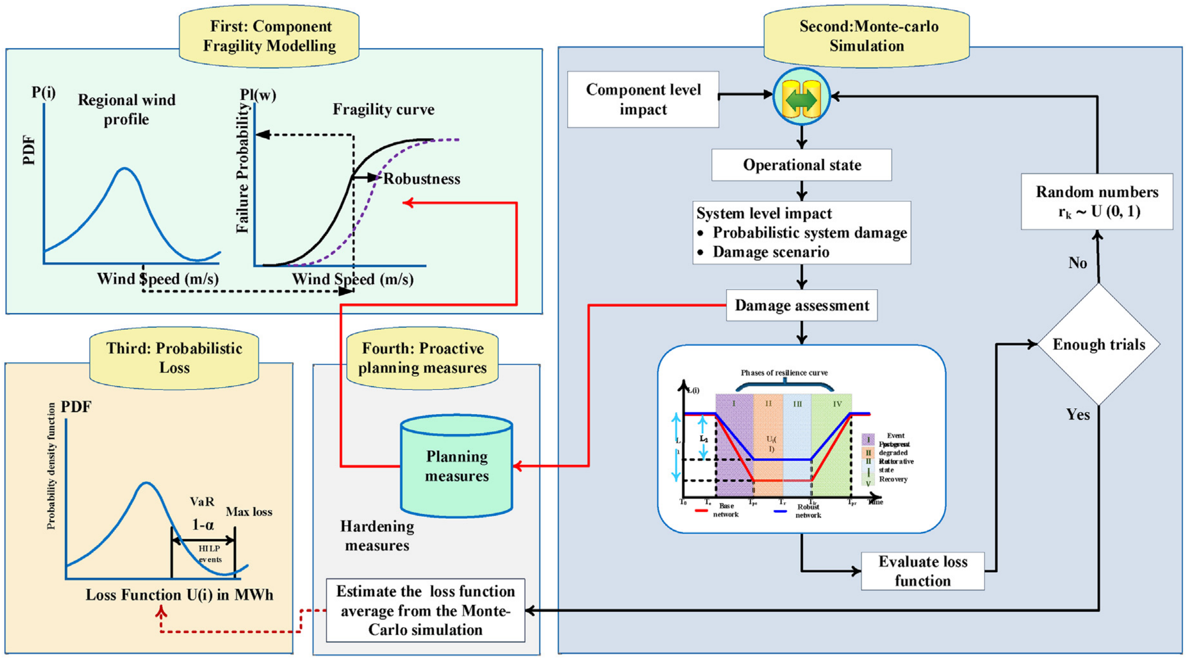

Fig. 8. The procedures for computing resilience metrics.

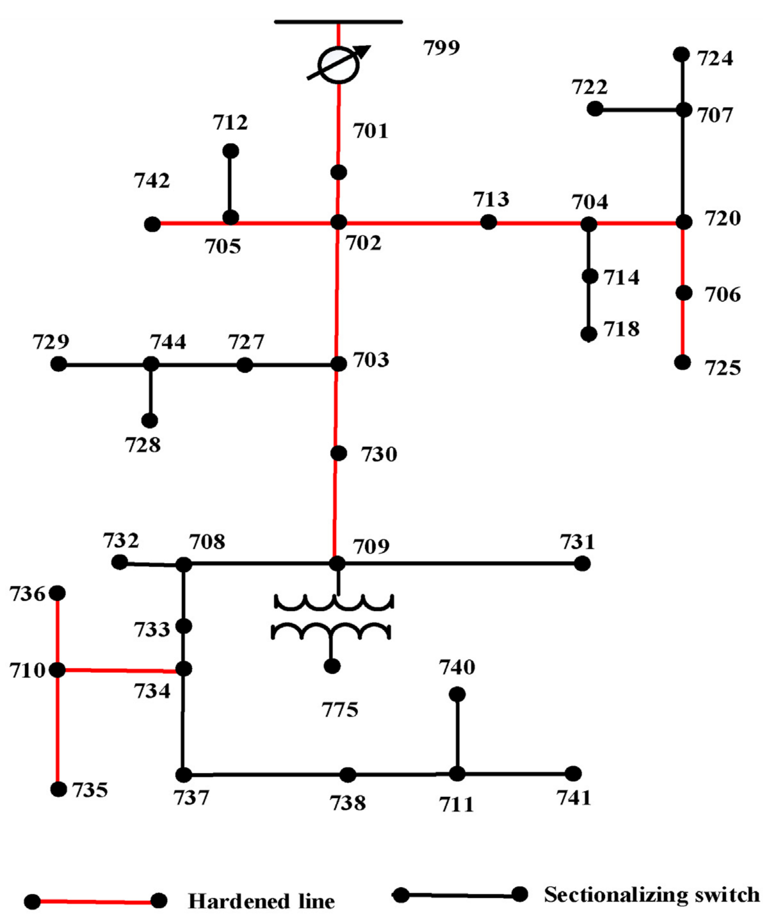

Fig. 9. IEEE 37-bus test system.

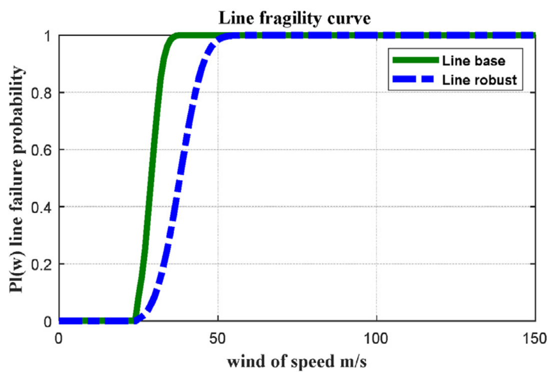

Fig. 10. Transmission line and tower wind fragility curves (base and robust case studies).

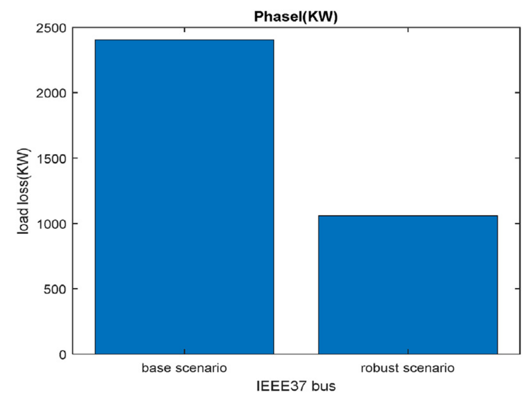

Fig. 12. Wind speed of 30 m/s resilience indicator for base and robust cases.

(4) It is important to keep in mind that the time period of Phase I is identified and presumed to be 2 h in this study. For all simulations, a risk threshold of = 0.95 is chosen (Bardou et al., 2009).

First, a sample of wind speed with the PDF for the regional profile (as shown in Fig. 2) is assumed and then the failure probability for the power system infrastructures (towers, lines, and transformers) is computed. The number of trials required for the convergence of the network loss function for a certain damage situation is calculated using a number of Monte Carlo calculations. For the sampled wind speed, about 1000 trials are sufficient to achieve convergence in both cases. Each trial's loss function is determined by analyzing the resilience curve's phases. Finally, the 1000 Monte Carlo runs' resulting loss functions are then averaged. By choosing multiple wind speeds from the PDF, the procedure is repeated for the given profile of wind speed. This aids in modeling the system's reaction to various weather occurrence severity (extreme, high, and normal).

7.3. Assessing the effects of wind speed on operational resilience

Fig. 10 depicts wind fragility curves for transmission lines (base and robust case studies). The convergence of 1000 Monte Carlo simulations for a variety of circumstances in the IEEE 37-bus are seen in Fig. 11 for two separate phases (base and robust) under extreme wind scenarios for different scenarios. The failure probability of distribution lines during the event of high-speed wind is decreased by reinforcing a few distribution lines, which lowers the load loss (kW) in Phase I. The system load loss (MW) for the basic and robust network is explored and depicted in Fig. 12 for the IEEE 37-bus test case.

7.4. Risk-based resilience metric calculation

As explained before, VaRα indicates the largest probable loss, whereas CVaRα measures the projected deficit owing to the most influence occurrences that exceed a particular level of risk. These measures are acceptable options for assessing

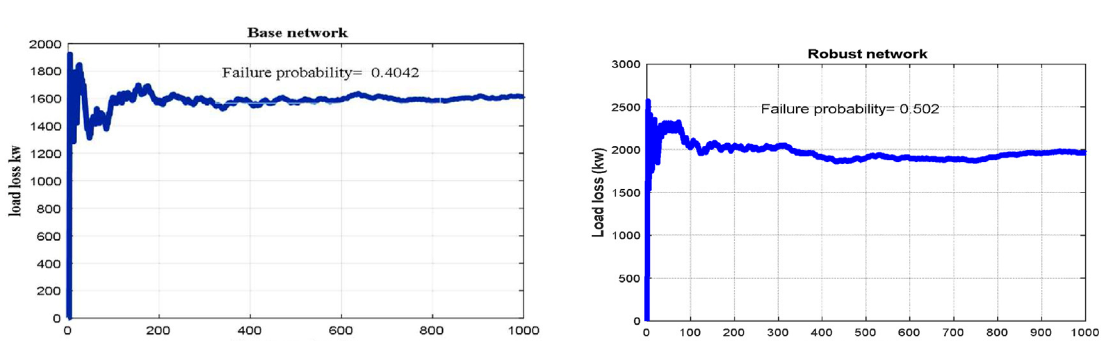

Fig. 11. Monte Carlo simulations convergence for several situations in IEEE 37-bus after 1000 attempts.

Table 1. VaRα and CVaRα for various wind scenarios for IEEE 37-bus with α = 95%.

Weather scenario	VaRα (MWh)	CVaRα (MWh)
Normal	3.025	3.658
High	14.359	19.537
Extreme	69.159	100.68

Table 2. VaRα and CVaRα for different cases with α = 95%.

Network	VaRα (MWh)	CVaRα (MWh)
Base network	69.159	100.68
Robust network	51.616	85.966

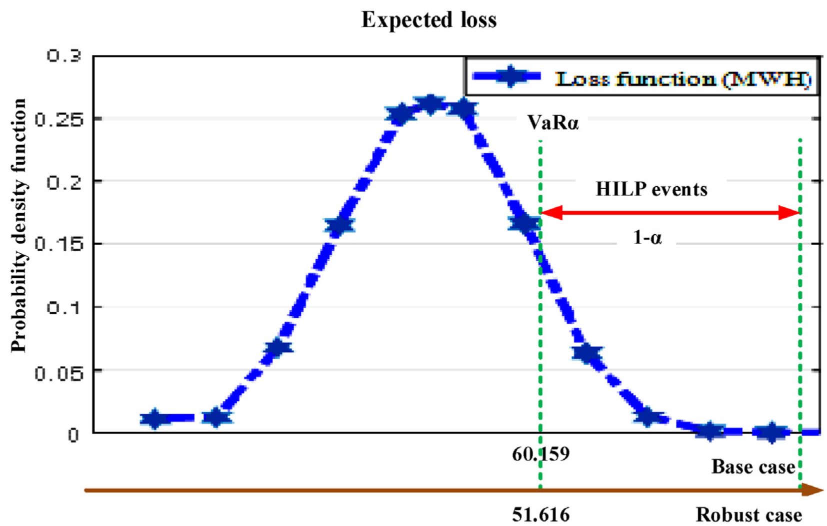

Fig. 13. The PDF of expected loss for the test case under the severe wind profile for the base and robust networks.

operational resilience since they precisely estimate severe losses due to low-frequency events. Two case studies will be considered:

(1) Base case: This scenario assumes a base case system without any reinforced lines or sophisticated restoration techniques. The VaRα and CVaRα for each of the three wind profiles (Extreme, high, and normal) are listed in Table 1. The results prove that an extreme wind profile results in a larger predicted resilience loss (MWh) than a normal wind profile. It is 100.68 MWh compared with 3.658 MWh for both the extreme and normal weather scenarios, respectively as measured by CVaRα.

(2) Robust case: In this case, 15 distribution lines are randomly chosen and hardened for the studied IEEE 37-bus test system. The values for VaRα and CVaRα are shown in Table 2 for base and robust cases. These results prove that VaRα and CVaRα values for the robust case are lower than for the base case. There is an improvement of 68.412% in VaRα and 99.83% in CVaRα. Note that, the authors only considered the extreme wind profile when assessing the resilience values for the test cases.

The performance loss function (MWh) of the system for the base and robust networks for the IEEE 37-bus test system under the severe wind profile is shown in Fig. 13. From these results it can see how well the suggested method can measure the resilience to weather events for particular geographic locations.

8. Conclusion

This paper introduced a probabilistic method to measure the resilience of a distribution power system exposed to HILP events. The study was based on two measures indicators, VaRα which measures maximum probable loss, and CVaRα which evaluates the anticipated decrease caused by the events with the biggest impact that occur above a specified risk threshold, α. The effects of HILP events on distribution network performance were evaluated. Similarly, the dangers these occurrences represent to the system's resilience were quantified, using a framework based on the Monte Carlo simulation method. In which the Monte Carlo simulation is used to generate damage scenarios, develop system-level impact, and calculate the load loss for each weather event. The effects of storms or any other heavy calamities on electric networks are estimated using component-level fragility curves.

The paper properly reflected and discussed a method for computing the outcomes of robust techniques for enhancing the resilience of electrical distribution systems. Thereby it decreases the probable loss and increases the system resilience. According to the study results, the robust case's VaRα and CVaRα values are lower than those of the basic case. VaRα and CVaRα both show improvements of 68.412% and 99.83%, respectively. The proposed method can help planners to predict and appropriate system infrastructure upgrades that can reduce the impact of a forthcoming extraordinary circumstance on the system's important loads.

Future work may also cover the following topics: (i) assessing the time for the system to repair, (ii) investigating the impact of using load-shedding programs, (iii) enhancing Grid Resilience with Integrated Storage from Electric Vehicles for critical load restoration, and (iv) optimal planning of resilience strategies under a limited investment budget.

Author contributions statement

Enas Hegazy: Data curation, Writing-Original draft preparation, Resources; Abdelfattah Eladl: Conceptualization, Methodology, Visualization, Validation; Magdi El-Saadawi: Investigation, Supervision, Writing-Reviewing, Editing the Manuscript.

Conflicts of interest

The authors declare that they have no known competing financial interests or personal relationships that could have appeared to influence the work reported in this paper.

References

Applied Technology Council, Dec. 2018. Seismic Performance Assessment of Buildings Volume 1—Methodology. Redwood, CA, USA. ATC-58-175.

Arghandeh, R., Meier, A., Mehrmanesh, L., Mili, L., 2016. On the definition of cyber-physical resilience in power systems. Renew. Sustain. Energy Rev. 58, 1060−1069.

Bardou, O., Frikha, N., Pages, G., 2009. Computing VaR and CVaR using stochastic approximation and adaptive unconstrained importance sampling. Monte Carlo Methods Appl. 15, 173−210.

Brown, H., Suryanarayanan, S., Natarajan, S., Rajopadhye, S., 2012. Improving reliability of islanded distribution systems with distributed renewable energy resources. IEEE Trans. Smart Grid 3, 2028−2038.

Chen, B., Chen, C., Wang, J., Butler-Purry, K.L., 2018. Sequential service restoration for unbalanced distribution systems and microgrids. IEEE Trans. Power Syst. 33, 1507−1520.

China Meteorological Data System, 2020 (Online. URL:).

Coffey, B., Stern, A., Wing, I., 2015. Climate Change Impacts on Us Electricity Demand: Insights from Micro-consistent Aggregation of a Structural Model,‘ International Energy Workshop. University of South Carolina.

Corporation, ReliaSoft, 2015. Life Data Analysis Reference. Tools to Empower Reliability Professional.

Dalton, M., Mote, P., 2013. Climate Change in the Northwest. Island Press, Washington, DC, USA, pp. 41−66.

Dunn, S., Galasso, C., Wilkinson, S., Manning, L., Alderson, D., 2015. Development of empirical fragility curves for electrical supply systems subjected to wind hazard. In: Proc 12th Int Conf Appl Statist Probab Civil Eng, pp. 3343−3362.

Executive Office of the President of the United States, 2013. Economic Benefits of Increasing Electric Grid Resilience to Weather Outages.

Fang, Y., Sansavini, G., Zio, E., 2019. An optimization-based framework for the identification of vulnerabilities in electric power grids exposed to natural hazards. Soc. Risk Anal. 39, 1949−1969.

Fisher, R., et al., 2010. Constructing a Resilience Index for the Enhanced Critical Infrastructure Protection Program. Argonne National Laboratory, Chicago, IL, USA.

Friederike, E., et al., 2022. Climate Change Increased Rainfall Associated with Tropical Cyclones Hitting Highly Vulnerable Communities in Madagascar, Mozambique & Malawi. Grantham Institute, London, UK. Imperial College.

Friedman, K., Hoffman, P., Bryan, W., 2012. Large Power Transformers and the US Electric Grid. The US Department of Energy.

Gholami, A., Shekari, T., Amirioun, M., Aminifar, F., Amini, M., Sargolzaei, A., 2018. Toward a consensus on the definition and taxonomy of power system resilience. IEEE Access 6, 32035−32053.

Harrison, R., 2010. Introduction to Monte Carlo simulation. In: AIP Conference Proceedings, vol. 1204. American Institute of Physics, pp. 17−21 (1).

Ji, C., Wei, Y., Poor, H.V., 2017. Resilience of energy infrastructure and services: modeling, data analytics, and metrics. Proc. IEEE 105, 1354−1366.

Johnston, P.C., 2012. Climate risk and adaptation in the electric power sector, Asian Develop. Bank, Mandaluyong, Philippines. Tech. Rep. https://www.adb.org/sites/default/files/publication/29889/climate-risks-adaptation-power-sector.pdf.

Kasakove, S., 2021. ‘We're Used to It’: Outside New Orleans and Still in the Dark,. The New York Times, 19 Sep, A15(L), available: https://link.gale.com/apps/doc/A675998885/AONE?u=anon~abdea80b&sid=googleScholar&xid=4ab7e896 [accessed 28 Apr 2023].

Kaygusuz, A., Alagoz, B., Akcin, M., Keles, C., Karabiber, A., Gul, O., 2014. Monte Carlo simulation-based planning method for overload safe electrical power systems. J. Electr. Eng. 14, 328.

Khodaei, A., 2014. Resiliency-oriented microgrid optimal scheduling. IEEE Trans. Smart Grid 5, 1584−1591.

Kirsty, M., Bell, K., 2014. Wind-related faults on the GB transmission network. Proc Int Conf Probabilistic Methods Appl Power Syst 1−6.

Lei, S., Wang, J., Chen, C., Hou, Y., 2018. Mobile emergency generator pre-positioning and real-time allocation for resilient response to natural disasters. IEEE Trans. Smart Grid 9, 2030−2041.

Li, W., Billinton, R., 2013. Reliability Assessment of Electric Power Systems Using Monte Carlo Methods. Springer, New York, NY, USA.
Liang, X., Goel, L., 1997. Distribution system reliability evaluation using the Monte Carlo simulation method. Elec. Power Syst. Res. 40, 75−83.
Lin, Y., Bie, Z., 2018. Tri-level optimal hardening plan for a resilient distribution system considering reconfiguration and DG islanding. Appl. Energy 210, 1266−1279.
Liu, C., 2015. Distribution systems: reliable but not resilient? [In my view]. IEEE Power Energy Mag. 13, 93−96.
Lopez, J., Franco, J., Rider, M., 2016. Optimization-based switch allocation to improve energy losses and service restoration in radial electrical distribution systems, IET Gener. Transm. Distrib. 10, 2792−2801.
MacKenzie, C., Zobel, C., 2016. Allocating resources to enhance resilience, with application to superstorm sandy and an electric utility. Risk Anal. 36, 847−862.
McGranaghan, M., Olearczyk, M., Gellings, C., 2013. Enhancing Distribution Resiliency: Opportunities for Applying Innovative Technologies. Electric Power Research Institute (EPRI), Palo Alto, CA, USA.
Melchor-Hernández, C., Rivas-Dávalos, F., Maximov, S., Coria, V., Moreno-Goytia, E., 2015. An analytical method to estimate the Weibull parameters for assessing the mean life of power equipment. Int. J. Electr. Power Energy Syst. 64, 1081−1087.
Nazemi, M., Moeini-Aghtaie, M., Fotuhi-Firuzabad, M., Dehghanian, P., 2020. Energy storage planning for enhanced resilience of power distribution networks against earthquakes. IEEE Trans. Sustain. Energy 11, 795−806.
Networks Association, Energy, 2011. Electricity networks climate change adaptation report. Tech. Rep. 1.
Obama, B., 2013. Critical Infrastructure Security and Resilience (Presidential Policy Directive/PPD-21). USAThe White House, Washington, DC.
Overbye, T., Cardell, J., Dobson, I., Kezunovic, M., Sen, P., Tylavsky, D., 2007. The Electric Power Industry and Climate Change: Power Systems Research Possibilities. In: Power Syst. Eng. Res. Center, Madison, WI, USA, pp. 7−16.
Panteli, M., Mancarella, P., 2017. Modeling and evaluating the resilience of critical electrical power infrastructure to extreme weather events. IEEE Syst. J. 11, 1733−1742.
Panteli, M., Mancarella, P., Trakas, D., Kyriakides, E., Hatziargyriou, N., 2017a. Metrics and quantification of operational and infrastructure resilience in power systems. IEEE Trans. Power Syst. 32, 4732−4742.
Panteli, M., Pickering, C., Wilkinson, S., Dawson, R., Mancarella, P., 2017b. Power system resilience to extreme weather: fragility modeling, probabilistic impact assessment, and adaptation measures. IEEE Trans. Power Syst. 32, 3747−3757.
Parhizi, S., Lotfi, H., Khodaei, A., Bahramirad, S., 2015. State of the art in research on microgrids: a review. IEEE Access 3, 890−925.
Paul, S., Padhy, N., 2019. Resilient scheduling portfolio of residential devices and plug-in electric vehicle by minimizing conditional value at risk. IEEE Trans. Ind. Inf. 15, 1566−1578.
Porter, K., Hamburger, R., Kennedy, R., 2007. Practical development and application of fragility functions. Struct. Eng. Res. Front. 1−16.
Ridwan, M., Talib, M., Ghazali, Y., March 2014. Application of Weibull-Bayesian for the Reliability Analysis of Distribution Transformers, IEEE 8th International Power Engineering and Optimization Conference, pp. 297−302.
Rockafellar, R., Uryasev, S., 2000. Optimization of conditional value-at-risk. J. Risk 2, 21−42.
Stankovic, A., 2018. The Definition and Quantification of Resilience. NJ, USA: IEEE PES Industry Technical Support Task Force, Piscataway.
Vugrin, E., Castillo, A., Silva-Monroy, C., 2017. Resilience metrics for the electric power system: a performance-based approach. Albuquerque, NM, USA. Tech. Rep.: Sandia Nat. Lab. https://www.osti.gov/servlets/purl/1367499/.
Wang, Z., Wang, J., 2015. Self-healing resilient distribution systems based on sectionalization into microgrids. IEEE Trans. Power Syst. 30, 3139−3149.